




ORIGINAL RESEARCH

# Chymase Inhibition Resolves and Prevents Deep Vein Thrombosis Without Increasing Bleeding Time in the Mouse Model

Catherine Lapointe , BSc; Laurence Vincent , MSc; Hugo Giguère , PhD; Mannix Auger-Messier , PhD; Adel Schwertani , PhD; Denan Jin , MD, PhD; Shinji Takai , PhD; Gunnar Pejler , PhD; Martin G. Sirois , PhD; Hanna Tinel , PhD; Stefan Heitmeier , PhD; Pedro D'Orléans-Juste , PhD

**BACKGROUND:** Deep vein thrombosis (DVT) is the primary cause of pulmonary embolism and the third most life-threatening cardiovascular disease in North America. Post-DVT anticoagulants, such as warfarin, heparin, and direct oral anticoagulants, reduce the incidence of subsequent venous thrombi. However, all currently used anticoagulants affect bleeding time at various degrees, and there is therefore a need for improved therapeutic regimens in DVT. It has recently been shown that mast cells play a crucial role in a DVT murine model. The underlying mechanism involved in the prothrombotic properties of mast cells, however, has yet to be identified.

**METHODS AND RESULTS:** C57BL/6 mice and mouse mast cell protease-4 (mMCP-4) genetically depleted mice (mMCP-4 knockout) were used in 2 mouse models of DVT, partial ligation (stenosis) and ferric chloride–endothelial injury model of the inferior vena cava. Thrombus formation and impact of genetically repressed or pharmacologically (specific inhibitor TY-51469) inhibited mMCP-4 were evaluated by morphometric measurements of thrombi immunochemistry (mouse and human DVT), color Doppler ultrasound, bleeding times, and enzymatic activity assays ex vivo. Recombinant chymases, mMCP-4 (mouse) and CMA-1 (human), were used to characterize the interaction with murine and human plasmin, respectively, by mass spectrometry and enzymatic activity assays. Inhibiting mast cell-generated mMCP-4, genetically or pharmacologically, resolves and prevents venous thrombus formation in both DVT models. Inferior vena cava blood flow obstruction was observed in the stenosis model after 6 hours of ligation, in control- but not in TY-51469–treated mice. In addition, chymase inhibition had no impact on bleeding times of healthy or DVT mice. Furthermore, endogenous chymase limits plasmin activity in thrombi ex vivo. Recombinant mouse or human chymase degrades/inactivates purified plasmin in vitro. Finally, mast cell–containing immunoreactive chymase was identified in human DVT.

**CONCLUSIONS:** This study identified a major role for mMCP-4, a granule-localized protease of chymase type, in DVT formation. These findings support a novel pharmacological strategy to resolve or prevent DVT without affecting the coagulation cascade through the inhibition of chymase activity.

**Key Words:** chymase ■ deep vein thrombosis ■ mouse mast cell protease-4 knockout ■ mouse ■ plasmin ■ TY-51469

**D**eep vein thrombosis (DVT), a major cause of venous thromboembolism, is commonly associated with “flow-impeding” clots located predominantly in major veins.<sup>1,2</sup> DVT in humans requires medical consultation with rapid diagnosis and potential therapy, to

reduce the risk of complications, such as pulmonary embolism or post-thrombotic syndrome.<sup>3</sup> Numerous risk factors, such as cancer or cancer therapy, aging, obesity, diabetes, smoking, pregnancy, birth control medications, defective coagulation system, and family

Correspondence to: Pedro D'Orléans-Juste, PhD, Department of Pharmacology and Physiology, Université de Sherbrooke, 3001, 12<sup>e</sup> Avenue Nord, Sherbrooke, QC J1H 5N4, Canada. Email: [labpdj@usherbrooke.ca](mailto:labpdj@usherbrooke.ca)

Supplemental Material is available at <https://www.ahajournals.org/doi/suppl/10.1161/JAHA.122.028056>

For Sources of Funding and Disclosures, see page 12.

© 2023 The Authors. Published on behalf of the American Heart Association, Inc., by Wiley. This is an open access article under the terms of the [Creative Commons Attribution-NonCommercial-NoDerivs](#) License, which permits use and distribution in any medium, provided the original work is properly cited, the use is non-commercial and no modifications or adaptations are made.

JAHA is available at: [www.ahajournals.org/journal/jaha](http://www.ahajournals.org/journal/jaha)

## CLINICAL PERSPECTIVE

### What Is New?

- The chymase-specific inhibitor TY-51469 resolves or prevents venous thrombi in a stenosis model and reduces ferric chloride–induced thrombus formation in the mouse inferior vena cava.
- Inhibition of chymase does not impact bleeding times or coagulation in wild-type mice.
- Chymase reduces plasmin activity within thrombi of deep vein thrombosis mice.
- Human chymase immunoreactivity is localized in thrombi from patients with deep vein thrombosis, and recombinant human chymase hydrolyzes specific peptide bonds within the active site of plasmin, thus inhibiting its activity *in vitro*.

### What Are the Clinical Implications?

- Bleeding observed with current anticoagulant therapies remains a common complication.
- The present study suggests that inhibition of intrathrombus-located chymase is a new profibrinolytic strategy with no impact on hemostasis.
- This is also the first nontissue plasminogen activator–dependent strategy to pharmacologically resolve already formed thrombi in an experimental model of inferior vena cava stenosis.

## Nonstandard Abbreviations and Acronyms

<b>CMA-1</b>	human chymase
<b>FeCl<sub>3</sub></b>	ferric chloride
<b>IVC</b>	inferior vena cava
<b>mMCP-4</b>	mouse mast cell protease-4
<b>rCMA-1</b>	recombinant human chymase
<b>rmMCP-4</b>	recombinant mouse mast cell protease-4
<b>WT</b>	wild type

genetics, are involved in the incidence and severity of the disease.<sup>1,3,4</sup> Health care costs associated with DVT and pulmonary embolism annually exceed \$10 billion in the United States.<sup>5</sup>

A suspicion of a DVT by health care professionals is commonly confirmed by ultrasound imaging of the affected area and by measuring plasma concentrations of D-dimer, a marker for polymeric fibrin degradation complexes.<sup>6</sup> Appropriate treatment strategies are often implemented according to a risk assessment model to adapt a treatment regimen to the risk level of the

patient. It can be either limited to 3 months to reduce the existing thrombus burden or indefinitely prolonged to reduce the risk of recurrent events as well as the risk of more severe complications, such as pulmonary embolism.<sup>6</sup> Low-molecular-weight heparins, such as enoxaparin, vitamin K antagonists, such as warfarin, and direct oral anticoagulants, such as rivaroxaban or apixaban, are indicated and recommended for the treatment or prevention of DVT, depending on different factors.<sup>2,6,7</sup> However, these medications share important limitations. As anticoagulants, they are thought to act indirectly on the degradation of fibrin by shifting the balance between coagulation and fibrinolysis in favor of the latter, which requires extended time and is less efficient in comparison with direct resolution of clot material. Irrespective of their exact mechanisms of action however, intake of all of these anticoagulants leads to increased bleeding risks.<sup>2,7,8</sup>

Although thrombolytics, such as tPA (tissue-type plasminogen activator), may dissolve clots directly and more effectively, increase the patency of the veins, and reduce the incidence of post-thrombotic syndrome in clinical studies, higher risks for bleeding complications are prevalent, strongly limiting the target population to patients fulfilling strict eligibility criteria.<sup>9,10</sup> In addition, treatment with thrombolytics is limited to the hospital setting. Thus, there is still a high medical need for efficacious and safe dissolution strategies of thrombi in veins.

Recently, Ponomaryov et al reported that mast cells are dynamically involved in the formation of DVT in a stenosis mouse model.<sup>11</sup> In support for this, mast cell–deficient Kit<sup>W/W-v</sup> or Kit<sup>W-sh/W-sh</sup> mice did not develop DVT after ligation of the inferior vena cava (IVC) when compared with wild-type (WT) mice.<sup>11</sup>

Derived from hematopoietic cells in the bone marrow as well as the spleen, mast cells circulate in the blood as precursors before homing to tissues where their maturation is completed. Mast cells may mature from resident precursors preexisting at different tissues, such as the heart,<sup>12,13</sup> lungs,<sup>14</sup> and blood vessels.<sup>15</sup> Growth factors, such as stem cell factor, are involved in the maturation of mast cells in selected tissues.<sup>16</sup> In humans and rodents, connective tissue and mucosal mast cells have been identified.<sup>17</sup> Increased mast cell numbers and densities are reported in myocardial failure, atherosclerosis, and ischemia, and mast cells are instrumental in transplant-related fibrosis.<sup>16,18,19</sup> Activated mast cells are involved in tissue repair and inflammatory processes, such as wound healing/fibrosis, cardiac remodeling, and angiogenesis.<sup>16,20–22</sup> Mast cells contain cytoplasmic granules, which, on stimulation, release several autacoids, cytokines, proteoglycans, and proteases, the latter including chymase, tryptase, cathepsin G, and carboxypeptidase A3.<sup>16</sup> Of relevance for the present study, mast cells are degranulated by hypoxia,

which also occurs in DVTs.<sup>23,24</sup> To date, only one single chymase,  $\alpha$ -chymase (human chymase [CMA-1]), has been reported in humans, whereas in mice, 4 major chymases are expressed, of which mouse mast cell protease-4 (mMCP-4) appears to be the functional ortholog to the human chymase (CMA-1).<sup>18</sup>

Over the past decades, several selective chymase inhibitors, such as TY-51469, have been developed and reported useful against cardiovascular diseases, such as atherosclerosis, heart failure, and myocardial infarction in animal models.<sup>18,25</sup> However, whether genetic repression or inhibition of mast cell–derived chymase also represses venous thrombus formation remains an open question. The latter issue will be addressed in this study, by using mouse models of venous thrombosis caused by either partial ligation of the IVC or ferric chloride ( $\text{FeCl}_3$ )–induced injury of the vascular wall.

Our results reveal that chymase inhibition may be a novel therapeutic target for efficacious and safe dissolution and prevention of venous thrombi.

## METHODS

See Data S1 for the Supplemental Methods. The authors declare that all supporting data and methods are available in the article (and its Supplemental Material). Data supporting the findings of this study are available from the corresponding author on reasonable request.

### Animals

C57BL/6 mice ( $n=225$ ) were purchased from Charles River (Montréal, QC, Canada), and the colonies were maintained and bred in our animal facilities. The mMCP-4 knockout mice ( $n=50$ ) were also bred as previously described.<sup>26</sup> The mMCP-4 knockout mice were backcrossed for >18 generations with C57BL/6 congeners and are therefore highly congenial with the later strain.<sup>26</sup> Female and male mice (aged 8–10 weeks; weight, 18–25 g) were used for the experiments. The animals' conditions were regulated at constant room temperature (23°C) and controlled humidity of 78%. They were also under a controlled cycle of light/dark (6 AM to 6 PM) with standard chow and tap water available ad libitum. Animal care and experimentations were performed in accordance with the *Guide for the Care and Use of Laboratory Animals*, as adopted and promulgated by the US National Institutes of Health, and were approved by the Ethics Committee on Animal Research of the Université de Sherbrooke in accordance with the guidelines of the Canadian Council on Animal Care.

### Drugs

The chymase inhibitor, TY-51469 (2-(4-((5-fluoro-3-methylbenzo[b]thiophene)-2-sulfonamido)-3-(methylsulfonyl)phenyl)thiazole-4-carboxylic acid), was

obtained from Toa Eiyo Limited (Osaka, Japan) and was dissolved in a vehicle solution of 0.025 M NaOH diluted in 10 mM PBS (pH 7.4). The plasmin/plasminogen inhibitor, BAY 1214237 (10-chloro-2-oxo-1,2-dihydropyrimido[1,2-b]indazol-4-yl) piperidinium chloride, was obtained from Bayer AG (Wuppertal, Germany) and was dissolved in 10 mM PBS (pH 7.4). BAY 1214237 inhibits human purified plasmin hydrolytic activity with a half maximal inhibitory concentration of 4.43  $\mu\text{M}$  (results not shown).

### Mouse $\text{FeCl}_3$ -Induced Endothelial Insult Model

The  $\text{FeCl}_3$ -injury model was performed as previously described.<sup>27</sup> WT male mice were treated with vehicle, TY-51469 (10 mg/kg), BAY 1214237 (1 mg/kg), or a coadministration of TY-51469 and BAY 1214237 (10 and 1 mg/kg, respectively) 1 hour before anesthesia with ketamine/xylazine (87/13 mg/kg intramuscular). A laparotomy was performed, and the guts were gently displaced without injury from the abdominal cavity and conserved in 0.9% NaCl solution (37°C). The IVC was exposed by separation of the vessel between the renal and ilio-lumbar veins. A 2×2-mm double-layered absorbent gauze saturated in 0.37 M (10% w/v in sterile water)  $\text{FeCl}_3$  (Sigma-Aldrich, St. Louis, MO) was applied directly on the isolated IVC for 3 minutes and then removed.<sup>27</sup> The guts were subsequently reinserted in their original location in the abdomen. Mice were euthanized 30 minutes later to access the thrombotic area in the IVC. IVCs were dissected and thrombi were isolated and weighted with an analytical balance (0.1 mg accuracy; Entris II; Sartorius).

### Ligation Surgery

As previously described by Ponomaryov et al and Canobbio et al,<sup>11,28</sup> stenosis of the IVC was performed in anesthetized mice (mixture of 2% isoflurane and 2.5% oxygen). A laparotomy was performed, and the guts were gently displaced without injury from the abdominal cavity and conserved in 0.9% NaCl solution (37°C). The IVC was exposed by isolating the vessel between the renal and ilio-lumbar veins. For partial ligation, a 30-G needle was used as a spacer. None of the side and back branches of the IVC was ligated.<sup>28</sup> After the ligation with polypropylene 7.0 sutures (FST, Foster City, CA) around both the IVC and the spacer, the latter was removed gently. The latter ensured that the endothelium is not denuded and that a residual flow of 10% in the IVC remains.<sup>11</sup> Guts were subsequently moved back in their original location in the abdomen, and the abdominal cavity was closed in layers with a braided 5.0 absorbable suture. The analgesia protocol was maintained for 24 hours after surgery with buprenorphine (0.1 mg/kg subcutaneous every

6–9 hours). The stenosis was evaluated 24 or 48 hours after ligation. The IVCs were dissected after euthanasia, and thrombi were isolated, measured, weighed, and finally stored at  $-80^{\circ}\text{C}$ .

### Preligation Treatment With TY-51469

Mice were pretreated with consecutive intraperitoneal doses of 10 mg/kg TY-51469,<sup>11,29</sup> according to the following scheme: 48 hours, 24 hours, and 30 minutes before IVC ligation. Animals were euthanized 24 hours after ligation. In a separate series of experiments, no differences in thrombus morphometrics (weight and length) were found in non-treated or vehicle-treated male (results not shown) female DVT mice (nonvehicle treated:  $6.1 \pm 0.98$  mg and  $3.69 \pm 0.58$  mm,  $n=10$ ; vehicle pretreated:  $5.78 \pm 0.77$  mg and  $3.79 \pm 0.67$  mm,  $n=6$ ).

### Postligation Treatment With TY-51469

Single doses of either vehicle or TY-1469 (0.1, 1, or 10 mg/kg) were administered intraperitoneally, 1, 6, or 24 hours after ligation of the IVC. Animals were euthanized 24 hours (for the 1 and 6 hours after ligation treatment) or 48 hours (for the 24 hours after ligation treatment) later to examine the thrombus formation.

### Tail-Bleeding Time

Mice were anesthetized with intramuscular ketamine/xylazine (87/13 mg/kg). A dose of 300 U/kg of unfractionated heparin (as specified by the manufacturer, Pfizer Canada Inc) or 10 mg/kg of TY-51469 was injected 1 hour before the test through the jugular vein or intraperitoneally, respectively. DVT mice were evaluated 24 hours after ligation, with or without a single dose of TY-51469 (10 mg/kg) 1 hour after ligation. Animals were then immobilized in a vertical position with their tail in a 2-mL tube filled with 1.5 mL Drabkin reagent (Sigma Aldrich Canada Co, Oakville, ON, Canada).<sup>30</sup> The tail was cut 3 mm starting from the extremity, and the time of bleeding cessation was noted. After 30 minutes, all animals were euthanized.<sup>30</sup>

### Murine Doppler Ultrasound

A high-frequency ultrasound imaging system (Vevo 3100; Fujifilm VisualSonics Inc) equipped with MX400 linear array transducer (40 MHz) was used to visualize by Doppler color blood flow mapping of the IVC and abdominal aorta in the stenosis mouse model of DVT. Female mice were anesthetized during the procedure (2% isoflurane; 98% oxygen; 1.5 L/min), and their abdomens were shaved and covered with ultrasound gel. Imaging of the vessels was performed 12 hours before ligation and 6 and 24 hours after ligation in female WT mice with or without 10 mg/kg TY-51469 1 hour after DVT. Following the last readings, the animals were

euthanized and examined for thrombi formation as well.

### Immunohistochemistry

Immunohistochemistry was performed on healthy and ligated IVC of WT and mMCP-4 knockout mice. Thrombus-containing vessels were fixed with 10% buffered formalin solution, processed, paraffin embedded, and finally sliced (4- $\mu\text{m}$  slice) at the service of the histopathology platform at Research Institute–McGill University Health Centre (Montréal, QC, Canada). Mast cells were stained with toluidine blue, and mMcp4 was detected using goat polyclonal anti-MCPT4 antibody (US Biological Life Science; catalog number M2414-20A; 1:400 dilution) and biotinylated horse anti-goat IgG (Vector Laboratories; catalog number BA9500; 1:200 dilution).

Human venous thrombi premade slides were obtained from Tissue for Research Ltd (Ellingham, Suffolk, UK). Mast cell chymase was detected using goat polyclonal IgG to human MCPT4 (Abcam; catalog number ab111239; 1:200 dilution).

### Plasmin Extraction ex Vivo

Plasmin-containing homogenates were extracted from thrombi of ligated WT mice. Thrombi were homogenized in 10 volumes (w/v) of 20 mM PBS (pH 7.4) supplemented with 1.5 mg/mL of BSA using a glass-Teflon homogenizer. The homogenates were transferred to 1 mL ultracentrifuge tubes and centrifuged at 100 000g for 20 minutes at  $4^{\circ}\text{C}$ .<sup>31</sup> Supernatants were kept at  $4^{\circ}\text{C}$  until they were tested for plasmin enzymatic activity the same day.

### Chymase Extraction ex Vivo

Chymase-containing homogenates were extracted from thrombi of ligated WT mice. Thrombi were homogenized in 10 volumes (w/v) of 20 mM PBS (pH 7.4) supplemented with 0.5 mg/mL of BSA using a glass-Teflon homogenizer.<sup>32</sup> The homogenates were centrifuged at 18 000g for 30 minutes at  $4^{\circ}\text{C}$ , and the supernatants were discarded. Pellets were then resuspended in the same initial volume of PBS. These last 2 steps were repeated 2 more times, except after the last centrifugation, supernatants were conserved.<sup>32</sup> Supernatants were subsequently maintained at  $4^{\circ}\text{C}$  until they were tested for chymase enzymatic activity on the same day following extraction.

### Measurement of Intrathrombus Plasmin or Chymase Enzymatic Activity

A total of 30  $\mu\text{L}$  of supernatants from thrombus extracts was used and placed directly in white 96-well plates. No variations in protein concentration per volume unit of thrombi were found using the Bradford



protein assay (result not shown). Some homogenates were treated with either vehicle or 10  $\mu$ M of TY-51469 (volume of 5  $\mu$ L) immediately before the fluorescence readings. A total of 65 to 70  $\mu$ L of 20 mM PBS (pH 7.4) supplemented with 1.5 mg/mL of BSA (for plasmin) or 0.5 mg/mL of BSA (for chymase) was added to each well to achieve a final volume of 100  $\mu$ L. Plasmin activity was determined by the hydrolysis rate of 50  $\mu$ M of the fluorogenic substrate, D-Ala-Leu-Lys-7-amino-4-methylcoumarin (Sigma Aldrich) at 37°C for 1 hour. Chymase activity was determined by the hydrolysis rate of 10  $\mu$ M of the fluorogenic substrate, Suc-Leu-Leu-Val-Tyr-7-amino-4-methylcoumarin (Peptide Institute Inc, Osaka, Japan) at 37°C for 1 hour. The fluorescence released was measured with an Infinite M1000 spectrophotometer (Tecan Austria GmbH, Grödig, Austria) with  $\lambda_{\text{ex}}$ =370 nm and  $\lambda_{\text{em}}$ =460 nm. A standard curve of 7-amino-4-methylcoumarin was also performed to quantify the concentration (nM) of the fluorogenic substrate cleavage.

## Statistical Analysis

All data are presented as the mean $\pm$ SEM. All statistical analyses were conducted using the GraphPad Prism 9 software (GraphPad Software, La Jolla, CA). Statistical significance was determined on the basis of 1-way ANOVA, followed by Bonferroni analysis (for multiple groups) or Mann-Whitney test (for comparison between 2 groups). Statistical significance was reached when the *P* value was <0.05, and 1 symbol (\*) denotes *P*<0.05, 2 symbols (\*\*) denote that *P*<0.01, and 3 symbols (\*\*\*) denote that *P*<0.001.

## RESULTS

### Short-Term Treatment With a Specific Chymase Inhibitor Prevents DVT Formation in WT Mice

Single-dose administration of TY-51469, a specific chymase inhibitor,<sup>18</sup> 1 hour post-ligation in the stenosis model reduced thrombus formation in a dose-dependent manner (Figure 1A and 1B; see experimental design in Figure S1). Both the weights and lengths of thrombi were reduced by >95% in TY-51469-treated male and female DVT mice at the dose of 10 mg/kg (Figure 1A and Figure S2A).

### No Changes in Hemostasis Are Observed in Chymase-Deficient Mice or WT Treated Mice With Chymase Inhibitor, TY-51469, in Vivo and in Vitro

Considering that the chymase inhibitor TY-51469 resolves or prevents IVC ligation-induced DVT, effects of

the chymase inhibitor or genetic chymase deficiency on hemostasis parameters were investigated in both male and female mice. Bleeding times were not increased in WT mice treated with the chymase inhibitor TY-51469 (10 mg/kg) or in mMCP-4 knockout mice of either sex (Figure 1C and Figure S2C). As a positive control, the bleeding times in mice treated with unfractionated heparin (300 U/kg) increased by 5-fold (25 $\pm$ 1.2 minutes) when compared with vehicle-treated WT control male (3.6 $\pm$ 0.8 minutes) (Figure 1C) or female mice (Figure S2C). Finally, prothrombin times as well as standard thromboelastographic parameters remained unchanged in blood recovered from WT mice treated with TY-51469, as well as in mMCP-4 knockout mice (Figures S2C and S3).

### Chymase Inhibition Allows Complete Venous Blood Flow in Ligated IVC of WT Mice

Next, were correlated, by laser Doppler-color mapping and blood velocity monitoring, the TY-51469-dependent reduction of thrombus size (Figure 1) with the restoration of IVC blood flow in the mouse stenosis model (Figure 2). DVT was associated with a marked increase in abdominal aortic flow<sup>33</sup> and full stasis of vena cava blood flow, from 6 to 24 hours after ligation (Table 1). In contrast, a single dose of TY-51469 (10 mg/kg, 1 hour after ligation) fully restored IVC blood flow in a sustained manner for at least 24 hours post-ligation in DVT mice (Figure 2 and Table 1). Furthermore, no changes were observed in the abdominal aortic flow in TY-51469-treated mice within the 24-hour time frame (Figure 2 and Table 1).

### mMCP-4 Knockout Mice Are Resistant to DVT Formation in the Stenosis Model

mMCP-4 is the main chymase expressed by connective tissue-type mast cells and is the functional ortholog to human chymase.<sup>26</sup> Next, we assessed whether genetic deficiency of chymase mMCP-4, similar to pharmacological chymase inhibition, affected DVT formation. Indeed, mMCP-4 knockout mice were found to be highly resistant to DVT formation after ligation in both male and female congeners (Figures 3A and S2A). Notably, only 5 of 31 tested male and female mMCP-4 knockout mice subjected to DVT developed morphometrically measurable thrombi.

### Chymase Inhibition Resolves Venous Thrombi in the Mouse Stenosis Model

To extend these findings, the impact of chymase inhibition as a preventive therapy for DVT was assessed by using a repetitive dose of 10 mg/kg of TY-51469 each day for 2 days, and on the same day as the

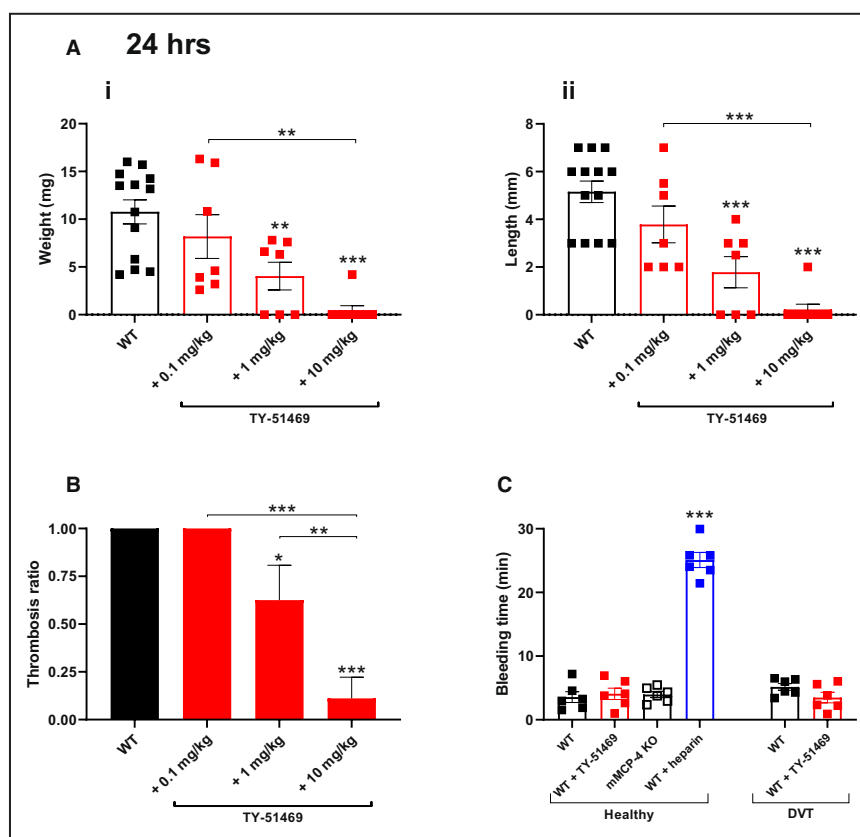


**Figure 1. Short-term single dose of TY-51469 protects against deep vein thrombosis (DVT) formation in a dose-dependent manner without bleeding adverse effects.**

**A**, Dose-dependent effect on the weight (mg; i) and length (mm; ii) of thrombi obtained 24 hours after DVT from inferior vena cava–ligated male wild-type (WT) mice treated with 0.1, 1, and 10 mg/kg chymase inhibitor TY-51469 1 hour post-ligation. **B**, Dose-dependent impact of chymase inhibitor TY-51469 on the thrombus incidence in WT mice. **C**, Bleeding times in male mice, as assessed by a tail-bleeding assay, reveal no difference between WT mice with or without 10 mg/kg TY-51469, in mouse mast cell protease-4 (mMCP-4) knockout (KO) mice, or DVT WT mice with or without 10 mg/kg TY-51469. The 300 U/kg heparin-treated WT mice were used as positive controls. Each group of mice represents the mean  $\pm$  SEM ( $n=6-13$ ). \* $P<0.05$ , \*\* $P<0.01$ , and \*\*\* $P<0.001$  compared with WT control group (asterisks directly placed over the error bar of each column); comparisons were also made between treated groups.

ligation surgery (see experimental design, Figure S1). By using this approach, similar results as for mMCP-4 knockout mice (either males or females) were obtained (Figures 3A and S2A). Furthermore, whether a single dose of 10 mg/kg of TY-51469 reduces mature venous thrombi was subsequently assessed. Indeed, WT mice treated with TY-51469, either 6 or 24 hours after ligation, displayed resolved thrombi, in both male and female mice (Figures 3A and 3B and S2A and S2B).

Similar to the stenosis model, it was observed in a  $\text{FeCl}_3$ -induced DVT model that a single dose of TY-51469 given 1 hour before venous damage in male WT mice reduced thrombus formation by 70% (Figure 3C). In agreement with the latter result, a similar reduction of thrombus size was observed in mice lacking mMCP-4 (Figure 3C).

## Mast Cell–Derived mMCP-4 Is Located Inside the Thrombus of WT Ligated IVC

To provide further insight into the role of chymase in regulation of thrombus formation during DVT, we next stained for mast cell (toluidine blue) and chymase immunoreactivity in IVCs of healthy and DVT mice. Toluidine blue–stained mast cells were identified in the adventitia of IVCs derived from both WT and mMCP-4 knockout mice (Figure 4). At 24 hours post-ligation, mMCP-4–specific immunoreactivity was localized in the periphery as well as within the occlusive thrombus in the IVC of WT mice (Figure 4) but not in thrombus-free veins isolated from IVC-ligated mMCP-4 knockout mice (Figure 4). Finally, toluidine blue and mMCP-4–specific immunoreactivity scores were quantified (Table S1) from the images of the 6 mouse vessels shown in Figure 4.

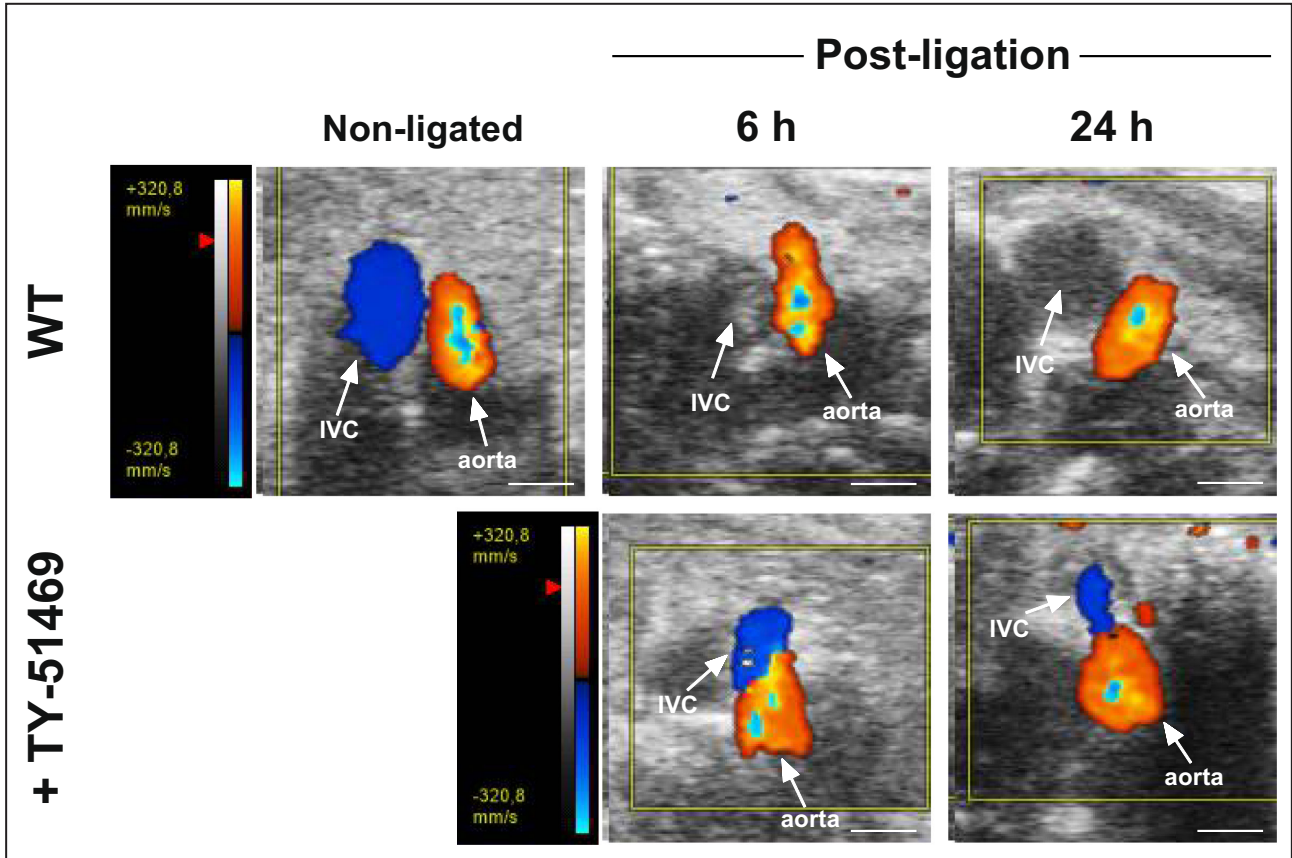


**Figure 2. Short-term chymase inhibition reinstates vena cava blood flow in deep vein thrombosis (DVT) mice.** Doppler color blood flow mapping of the inferior vena cava (IVC) and adjacent abdominal aorta (AA) in 8-week-old female mice. TY-51469 (10mg/kg) was administered intraperitoneally 1 hour after ligation. The image illustrates the apical view of the IVC and AA with the ultra-high-frequency linear array transducer (or scan head) tilted at an angle of 35±10 degrees from the posterior end of the mouse. DVT-induced IVC blood stasis in control WT mice 6hours after ligation. WT mice treated with TY-51469, 1 hour after ligation, show no variation in IVC and AA blood velocities when compared with the same animals before ligation. Control WT, unlike TY-51469–treated DVT mice, also showed compensatory increases in AA blood flow, 6 and 24 hours after ligation. The images are representative of 6 to 8 independent experiments. Bar=1 mm. WT indicates wild type.

### Mouse Chymase Inhibits Plasmin Activity in Vitro

Plasmin is the main fibrinolytic enzyme involved in the degradation of fibrin complexes in preformed thrombi.<sup>34</sup> We next assessed whether chymase can directly affect plasmin activity. Indeed, recombinant mMCP-4 induced a significant reduction of plasmin activity (measured as hydrolysis of a plasmin-specific fluorogenic substrate), and this effect of the murine

chymases was inhibited in a concentration-dependent manner by TY-51469 (Figure 5A).

### Intrathrombus Chymase Inactivates Plasmin Activity in a TY-51469–Sensitive Manner, ex Vivo

Enzymatic activity analyses showed that chymase is highly active in 24- and 48-hour-old thrombi, albeit to a lesser extent in the latter (Figure 5B and 5C).

**Table 1. Pulse-Wave Doppler Velocity Analysis**

Time after ligation, h	Abdominal aorta blood velocity, mm/s				Inferior vena cava blood velocity, mm/s			
	WT	No.	+10mg/kg TY-51469	No.	WT	No.	+10mg/kg TY-51469	No.
Nonligated	463.8±18.5	8	508.2±29.7	6	103.3±17.0	8	124.6±28.7	6
6	669.3±38.2 <sup>†</sup>	8	487.6±33.1	6	0±0 <sup>†</sup>	8	171.6±27.1	6
24	595.9±22.2 <sup>*</sup>	7	505.8±40.4	6	0±0 <sup>†</sup>	7	158.5±18.3	6

Each value represents the mean±SEM of 6 to 8 experiments. Statistical analysis: Mann-Whitney test. No, indicates number of experiments; and WT, wild type. <sup>\*</sup>P<0.05, <sup>†</sup>P<0.001 compared with the WT control group.

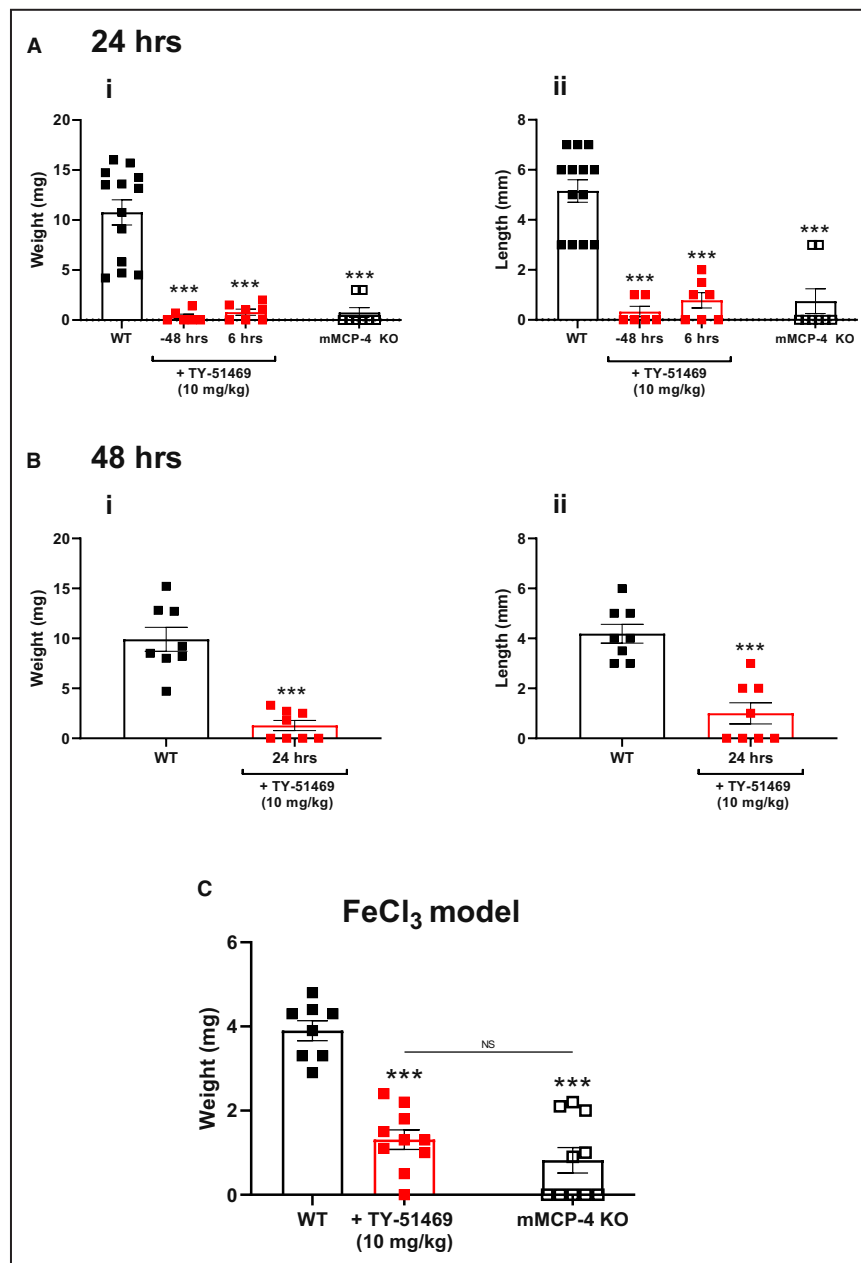


**Figure 3. Chymase inhibition protects against and resolves deep vein thrombosis in male mice in 2 murine models.**

Male wild-type (WT) mice were treated with 10mg/kg TY-51469 (intraperitoneally) (48 hours before and 6 or 24 hours after ligation), and mouse mast cell protease-4 (mMCP-4) knockout (KO) mice were subjected to an inferior vena cava stenosis for 24 (**A**) or 48 (**B**) hours. Morphometric parameters of thrombi were measured as weight (mg; **i**) and length (mm; **ii**). **C**, Weight of thrombi obtained after the ferric chloride insult model, 30 minutes after damage, from male WT mice treated with 10mg/kg TY-51469 and mMCP-4 KO mice. Each group represents the mean±SEM (n=6–12). \*\*\**P*<0.001 compared with the WT control group.

TY-51469 (10  $\mu$ M) abolished the chymase-like activity found in thrombi ex vivo (Figure 5C). In WT thrombi, an inverse correlation between chymase and plasmin enzymatic activities was observed at 24 and 48 hours post-IVC ligation. Moreover, TY-51469 (10  $\mu$ M) abolished chymase activity but conversely caused a robust

enhancement of plasmin activity (3.5-fold) in thrombi of WT mice (Figure 5B and 5C).

In a last series of in vivo experiments, the plasmin/plasminogen inhibitor BAY 1214237 (1 mg/kg) administered intraperitoneally, 1 hour prior to FeCl<sub>3</sub> application, fully reversed the inhibition of thrombus



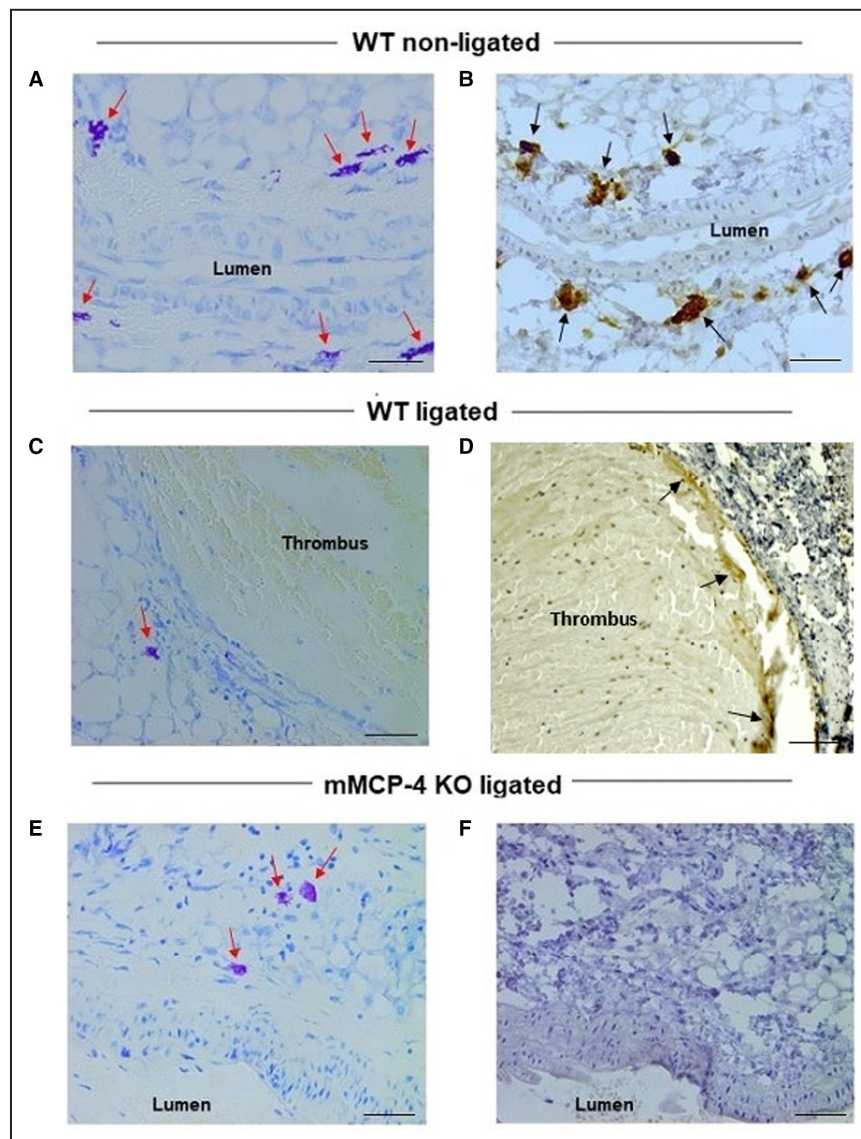


**Figure 4.** Mouse mast cell protease-4 (mMCP-4) immunoreactivity and toluidine blue (TB) mast cell staining in the inferior vena cava (IVC) of deep vein thrombosis mice.

**A**, TB staining of a nonligated IVC from a wild-type (WT) mouse. **B**, mMCP-4 immunoreactivity of a nonligated IVC from a WT mouse. **C**, TB staining of a ligated vein from a WT mouse. **D**, mMCP-4 immunoreactivity in a ligated IVC from a WT mouse (vessel lumen). **E**, TB staining of a ligated IVC from an mMCP-4 knockout mouse. **F**, Absence of mMCP-4 immunoreactivity in the same ligated IVC as in **E**. Dilution of the mMCP-4 antibody: 1:400. Red arrows: mast cells; black arrows: mMCP-4 immunoreactivity. The images are representative of 3 independent experiments. Bar=50  $\mu$ m.

formation induced by TY-51469 (10mg/kg, administered also 1 hour before chemical insult) in the mouse IVC (Figure S4).

### Chymase-Positive Mast Cells and CMA-1 Are Located Inside Thrombi of Patients With DVT

In 3 independent experiments, CMA-1–positive mast cells were identified within thrombi of human patient

left iliac, right femoral, and left groin varicose veins. Figure 6A depicts CMA-1–positive mast cells in the left groin varicose vein.

### Human Chymase Inhibits Plasmin Activity in Vitro

Similarly to mMCP-4, human recombinant chymase, CMA-1, induced a significant reduction of plasmin activity (measured as hydrolysis of a plasmin-specific fluorogenic

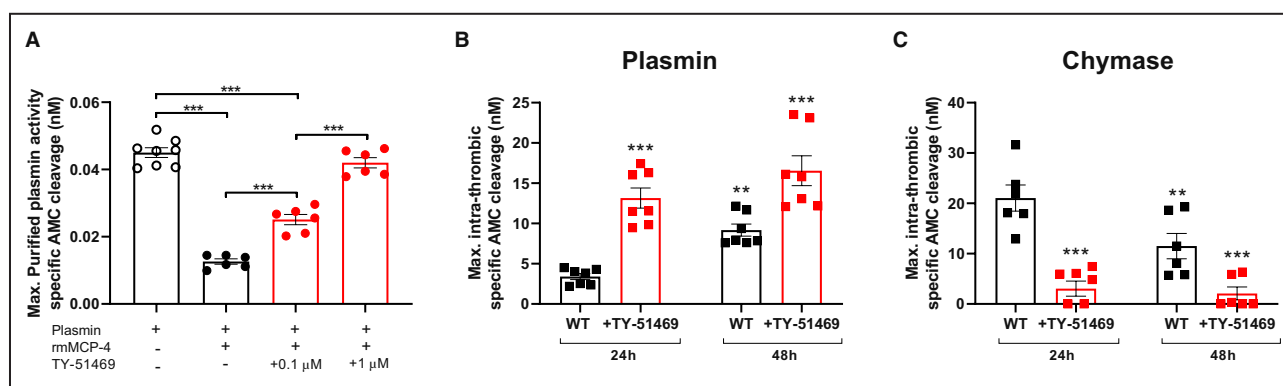


**Figure 5. Mouse mast cell protease-4 (mMCP-4) reduces plasmin activity within thrombi of deep vein thrombosis mice.**

**A**, Plasmin-like activity was measured in vitro using mouse purified plasmin incubated for 24 hours at 37°C with recombinant mMCP-4 with or without increasing concentrations of the chymase inhibitor TY-51469. **B** and **C**, Ex vivo enzymatic activity in thrombi harvested 24 or 48 hours after ligation from wild-type (WT) mice. WT thrombi were treated with vehicle or 10  $\mu$ M TY-51469 before the reading. **B**, Plasmin activity was measured as 7-amino-4-methylcoumarin (AMC)-specific cleavage (nM) of the fluorogenic substrate D-Ala-Leu-Lys-AMC. **C**, Chymase activity was measured as AMC-specific cleavage of the fluorogenic substrate Suc-Leu-Leu-Val-Tyr-AMC. Each bar represents the mean  $\pm$  SEM (n=6–8 independent experiments). \*\* $P$ <0.01, \*\*\* $P$ <0.001 compared with the plasmin only group or WT nontreated group. Max. indicates maximum.

substrate), and this effect was inhibited in a concentration-dependent manner by TY-51469 (Figure 6B). In addition, 6 cleavage sites of purified human plasmin by recombinant human chymase CMA-1<sup>35</sup> (yielding 5 distinct fragments; 4 of these within the catalytic pocket) were identified using trypsin digestion and cleavage product identification by liquid chromatography–tandem mass spectrometry (Table S2). This plasmin degradation was reduced in the presence of the chymase inhibitor, TY-51469 (Figure 6C and 6D). In agreement with the latter result, recombinant mMCP-4 also produced similar TY-51469-sensitive cleavage patterns for murine plasmin fragments (Figure S5A).

## DISCUSSION

Our study reports, for the first time, that mast cell-derived chymase plays a pivotal role in the stabilization of venous thrombi in mouse models by limiting the fibrinolytic efficacy of plasmin within the clot. Plasmin activity was impaired by chymase but was preserved by the chymase inhibitor TY-51469 in in vitro settings, both for recombinant human and mouse chymase as well as in mouse thrombi ex vivo. In agreement with this, chymase and chymase-positive mast cells were found within thrombi recovered from the mouse experiments as well as from patients with DVT. Importantly, mMCP-4 knockout mice or WT mice treated with TY-51469 did not display anticoagulant responses in ex vivo clotting time assays, nor was a prolongation in bleeding times observed when compared with control animals.

In the present study, we also demonstrate that chymase inactivates plasmin in the thrombus. Our results show that unlike current therapy for DVT, such as heparin, warfarin, or direct oral anticoagulants,<sup>2,7,36</sup>

inhibition of chymase did not affect the bleeding time in the tail vein model in mice, suggesting that inhibition of the mast cell endogenous serine protease does not influence hemostasis. More important, Ponomaryov et al also demonstrated that mast cell depletion abolishes DVT, with no impact on hemostasis and tail bleeding time in the mouse DVT model.<sup>11</sup>

Chymase released from mast cells is known to be rapidly neutralized in the blood by plasma protease inhibitors, such as  $\alpha$ -2-macroglobulin.<sup>37</sup> In this study, the tail-bleeding assay and thromboelastographic experiment demonstrate that circulating chymase at the bleeding site is not active, as previously reported for other large enzymes, such as plasmin.<sup>37</sup> However, our experiments suggest that intrathrombus chymase may be protected from protease inhibitors and, thereby, is capable of reducing plasmin activity via proteolysis. Together, our study thus introduces a novel role of chymase in the regulation of plasmin activity, specifically within the thrombotic microenvironment.

Fully formed thrombi are generated 3 to 6 hours after ligation in the IVC stenosis mouse model.<sup>38,39</sup> This model causes no direct endothelial damage in ligated veins and allows thrombus formation with a residual blood flow, thus closely mimicking the pathology in the large majority of clinical cases.<sup>38,40</sup> It is striking that the lack of mMCP-4 or administration of a chymase inhibitor 1, 6, or 24 hours after ligation is sufficient to prevent thrombus formation and, with regard to TY-51469, even dissolve already existing thrombi in the mouse model. Although this is similar to lytic effects of recombinant tPA (alteplase), chymase inhibition reveals no impact on bleeding time.<sup>41,42</sup> Furthermore, a single dose of TY-51469 in the stenosis mouse model preserves the IVC blood flow for 24 hours after ligation. In

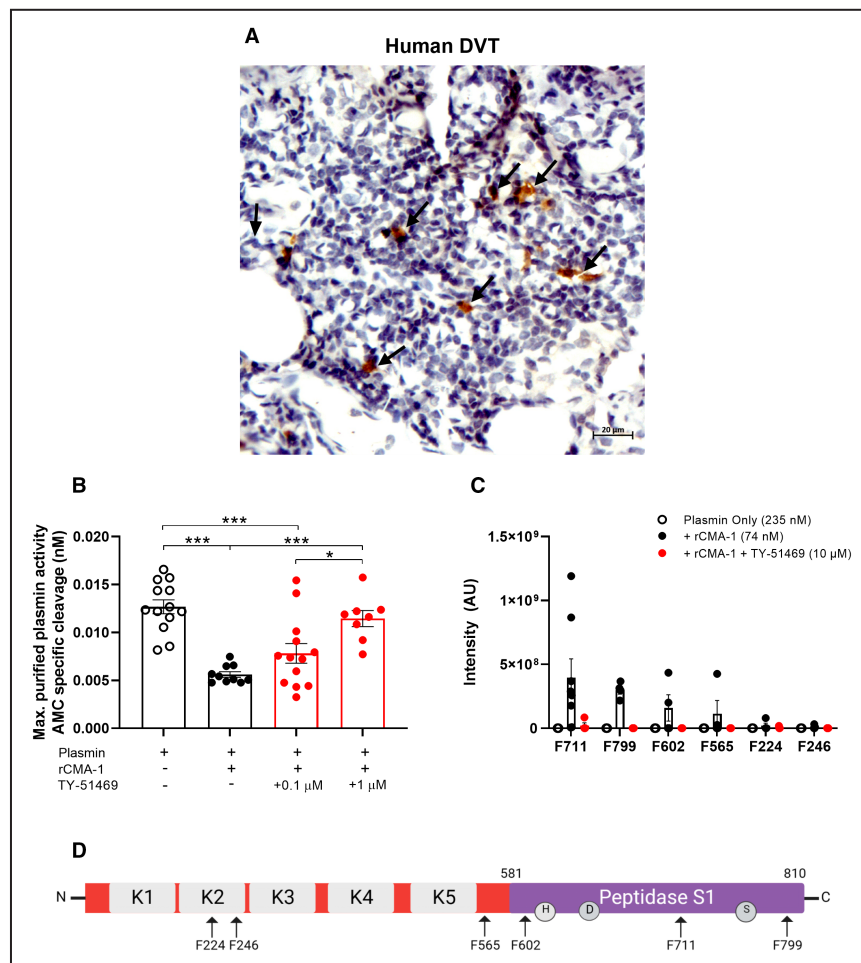


**Figure 6. Specific chymase immunostaining is found within human venous thrombi, and human recombinant chymase (rCMA-1) cleaves/inactivates human plasmin.**

**A**, Human deep vein thrombosis (DVT) samples show chymase immunoreactivity (brown) and chymase-positive mast cells inside the thrombi. Dilution of the CMA-1 antibody: 1 $\times$ 200; black arrows: CMA-1 immunoreactivity. The image is representative of independent experiments performed with venous thrombi extracted from 3 patients. Bar=20  $\mu$ m. **B**, Plasmin-like activity was measured in vitro with purified human plasmin incubated for 24 hours at 37°C with rCMA-1 with or without increasing concentrations of the chymase inhibitor TY-51469. Each bar represents the mean $\pm$ SEM (n=8–13). \* $P$ <0.05, \*\*\* $P$ <0.001. **C**, Identification of rCMA-1 cleavage sites in human plasmin using trypsin digestion and cleavage product identification by liquid chromatography–tandem mass spectrometry, represented as arbitrary intensity (4 samples tested). **D**, Schematic representation of human plasmin/plasminogen. rCMA-1 cleavage sites are indicated by black arrows. Created with [BioRender.com](https://www.biorender.com). AMC indicates 7-amino-4-methylcoumarin; AU, arbitrary unit; and Max., maximum.

clinical settings, a prompt blood flow restoration is also an indication of a reduced thrombus burden, reduced fibrosis of the vessel, and better outcome in reducing DVT complications in patients.<sup>43</sup>

In the present study, we also used a mouse model of FeCl<sub>3</sub>-induced DVT where the thrombus is provoked by an endothelial insult instead of blood stasis. As the Virchow triad describes, 3 factors are thought to contribute to thrombosis: hypercoagulability, blood stasis, and endothelial dysfunction. In conditions of vascular

insult, endothelial dysfunction occurs along with platelet activation, adhesion, and aggregation, followed by fibrin formation.<sup>44</sup> Interestingly, the present study shows that mMCP-4 knockout or WT mice treated with TY-51469 have reduced thrombus formation also in the FeCl<sub>3</sub>-induced endothelial insult model. In addition, the loss of antithrombotic properties of TY-51469 in IVC-FeCl<sub>3</sub> mice treated with the plasminogen/plasmin inhibitor BAY 1214237 further supports the profibrinolytic properties of chymase inhibitors in this mouse model



of venous thrombosis. Thus, this study shows that the impact of the chymase inhibitor TY-51469 is not limited to a single type of thrombosis pathogenesis, and chymase inhibition has therefore the potential to be effective in most clinical DVT scenarios.

Albeit the present study shows that a chymase inhibitor can resolve venous thrombi, a role for the latter serine protease in arterial thrombosis remains to be investigated. Ponomaryov et al did not report a significant role for mast cells in a mouse model of arterial thrombosis.<sup>11</sup> However, the FeCl<sub>3</sub>-injury experiments in mesenteric arteries performed by Ponomaryov and colleagues<sup>11</sup> were conducted in animals with healthy vessels, whereas it is well established that cardiovascular events in humans occur after plaque rupture or erosion of atherosclerotic arterial wall, which contains substantial amounts of mast cells.<sup>45</sup> Although showing large heterogeneity, arterial thrombi obtained from patients with stroke, myocardial infarction postmortem, or after thrombectomy are all known to be strongly dependent on fibrin formation. Therefore, a role for chymase in the pathologic features of arterial occlusion cannot be excluded, and chymase inhibition might have an impact as well. Finally, elevated D-dimer levels have previously been reported in the IVC stenosis mouse model.<sup>46</sup> Whether the antithrombotic effects afforded by mast cell depletion<sup>11</sup> or chymase inhibition are associated with reduced D-dimer levels in the mouse model requires further investigation.

Although we provide evidence that human chymase inactivates human plasmin within human venous thrombi, the strategy of using chymase inhibition in treatment of DVT in humans needs to be validated in clinical settings. Notably, the chymase inhibitor TY-51469 is not orally bioavailable and thus requires systemic administration. Future studies may require the use of novel orally available chymase inhibitors, such as fulacimstat (BAY-1142524).<sup>18,47–49</sup>

Altogether, the present in vivo and in vitro studies highlight the potential usefulness of chymase inhibition as a novel strategy for venous thrombus resolution without increasing bleeding risk.

## ARTICLE INFORMATION

Received October 15, 2022; accepted January 5, 2023.

### Affiliations

Department of Pharmacology and Physiology and Faculté de Médecine et des Sciences de la Santé (C.L., L.V., P.D.-J.) and Department of Medicine, Service of Cardiology, Faculté de Médecine et des Sciences de la Santé (H.G., M.A.-M.), Université de Sherbrooke, Sherbrooke, QC, Canada; Department of Medicine, McGill University, Montréal, QC, Canada (A.S.); Department of Innovative Medicine, Osaka Medical and Pharmaceutical University, Osaka, Japan (D.J., S.T.); Department of Medical Biochemistry and Microbiology, Uppsala University BMC, Uppsala, Sweden (G.P.); Montréal Heart Institute and Department of Pharmacology and Physiology, Université de Montréal, Montréal,

QC, Canada (M.G.S.); and Bayer AG, Research and Development, Pharmaceuticals, Wuppertal, Germany (H.T., S.H.).

### Acknowledgments

The authors thank Dr François-Michel Boisvert and Dominique Lévesque (Université de Sherbrooke) for the mass spectrometry experiments; Dr Dany Salvail (IPS-Thérapeutique, Sherbrooke, QC, Canada), Dr Sébastien Labbé (Immune Biosolutions Inc, Sherbrooke, QC, Canada), and Julie Brodeur (formerly from IPS-Thérapeutique) for the thromboelastographic experiments; Dr Bin Yu (McGill University, Montréal, QC, Canada) for the immunohistology experiments; Antoine Désilets (Université de Sherbrooke) for the spectrofluorometric experiments; and Dr Robert Day and Roxane Desjardins (Université de Sherbrooke) for the recombinant enzymes, human chymase (CMA-1) and recombinant mouse mast cell protease-4.

### Sources of funding

This project was supported by a grant (MOP-57883) from the Canadian Institutes for Health Research (Dr D'Orléans-Juste), the John E. Edwards Cardiology Chair (Dr D'Orléans-Juste), and the Réseau Québécois de Recherche sur les Médicaments (Drs D'Orléans-Juste and Sirois). C. Lapointe is the recipient of a doctorate studentship (Gérard-Eugène-Plante) from the Université de Sherbrooke. Dr Giguère was the recipient of a Natural Sciences and Engineering Research Council of Canada (Alexander-Graham-Bell) graduate scholarship–doctoral award (CGSD-504926). Dr Auger-Messier is supported by Fonds de Recherche du Québec-Santé research scholarship–career award (junior: 2–284164, 2020–2022; senior: 313286, 2022–2026). Drs Tinel and Heitmeier are employees of Bayer AG.

### Disclosures

C. Lapointe, L. Vincent, Dr Tinel, Dr Heitmeier, Dr Schwertani and Dr D'Orléans-Juste are inventors on a provisional patent related to this study.

### Supplemental Material

Data S1  
Tables S1–S2  
Figures S1–S5

## REFERENCES

- Heit JA. Epidemiology of venous thromboembolism. *Nat Rev Cardiol*. 2015;12:464–474. doi: 10.1038/nrcardio.2015.83
- McCullough M, Kholdani C, Zamanian RT. Prevention of deep vein thrombosis and pulmonary embolism in high-risk medical patients. *Clin Chest Med*. 2018;39:483–492. doi: 10.1016/j.ccm.2018.04.002
- Wenger N, Sebastian T, Engelberger RP, Kucher N, Spirk D. Pulmonary embolism and deep vein thrombosis: similar but different. *Thromb Res*. 2021;206:88–98. doi: 10.1016/j.thromres.2021.08.015
- Giustozzi M, Franco L, Agnelli G, Verso M. Unmet clinical needs in the prevention and treatment of cancer-associated venous thromboembolism. *Trends Cardiovasc Med*. 2022. doi: 10.1016/j.tcm.2022.02.003
- Grosse SD, Nelson RE, Nyarko KA, Richardson LC, Raskob GE. The economic burden of incident venous thromboembolism in the United States: a review of estimated attributable healthcare costs. *Thromb Res*. 2016;137:3–10. doi: 10.1016/j.thromres.2015.11.033
- Tritschler T, Kraaijpoel N, Le Gal G, Wells PS. Venous thromboembolism: advances in diagnosis and treatment. *JAMA*. 2018;320:1583. doi: 10.1001/jama.2018.14346
- McRae HL, Militello L, Refaai MA. Updates in anticoagulation therapy monitoring. *Biomedicine*. 2021;9:262. doi: 10.3390/biomedicine9030262
- Moia M, Squizzato A. Reversal agents for oral anticoagulant-associated major or life-threatening bleeding. *Intern Emerg Med*. 2019;14:1233–1239. doi: 10.1007/s11739-019-02177-2
- Powers WJ, Rabinstein AA, Ackerson T, Adeoye OM, Bambakidis NC, Becker K, Biller J, Brown M, Demaerschalk BM, Hoh B, et al. Guidelines for the early management of patients with acute ischemic stroke: 2019 update to the 2018 guidelines for the early management of acute ischemic stroke: a guideline for healthcare professionals from the American Heart Association/American Stroke Association. *Stroke*. 2019;50:e344–e418. Accessed March 31, 2022.
- Embersson J, Lees KR, Lyden P, Blackwell L, Albers G, Bluhmki E, Brott T, Cohen G, Davis S, Donnan G, et al. Effect of treatment delay, age,



- and stroke severity on the effects of intravenous thrombolysis with alteplase for acute ischaemic stroke: a meta-analysis of individual patient data from randomised trials. *Lancet*. 2014;384:1929–1935. doi: 10.1016/S0140-6736(14)60584-5
11. Ponomarev T, Payne H, Fabritz L, Wagner DD, Brill A. Mast cells granular contents are crucial for deep vein thrombosis in MiceNovelty and significance. *Circ Res*. 2017;121:941–950. doi: 10.1161/CIRCRESAHA.117.311185
  12. Janicki JS, Brower GL, Levick SP. The emerging prominence of the cardiac mast cell as a potent mediator of adverse myocardial remodeling. *Methods Mol Biol Clifton NJ*. 2015;1220:121–139. doi: 10.1007/978-1-4939-1568-2\_8
  13. Ngkelo A, Richart A, Kirk JA, Bonnin P, Vilar J, Lemitre M, Marck P, Branchereau M, Le Gall S, Renault N, et al. Mast cells regulate myofilament calcium sensitization and heart function after myocardial infarction. *J Exp Med*. 2016;213:1353–1374. doi: 10.1084/jem.20160081
  14. Bankova LG, Dwyer DF, Liu AY, Austen KF, Gurish MF. Maturation of mast cell progenitors to mucosal mast cells during allergic pulmonary inflammation in mice. *Mucosal Immunol*. 2015;8:596–606. doi: 10.1038/mi.2014.91
  15. Bot I, Shi G-P, Kovanen PT. Mast cells as effectors in atherosclerosis. *Arterioscler Thromb Vasc Biol*. 2015;35:265–271. doi: 10.1161/ATVBAHA.114.303570
  16. Krystel-Whittemore M, Dileepan KN, Wood JG. Mast cell: a multifunctional master cell. *Front Immunol*. 2016;6:620. doi: 10.3389/fimmu.2015.00620
  17. da Silva EZM, Jamur MC, Oliver C. Mast cell function: a new vision of an old cell. *J Histochem Cytochem*. 2014;62:698–738. doi: 10.1369/0022155414545334
  18. Pejler G. Novel insight into the in vivo function of mast cell chymase: lessons from knockouts and inhibitors. *J Innate Immun*. 2020;12:357–372. doi: 10.1159/000506985
  19. Kovanen PT. Mast cells: Multipotent local effector cells in atherothrombosis. *Immunol Rev*. 2007;217:105–122. doi: 10.1111/j.1600-065X.2007.00515.x
  20. Caughey GH. Mast cell proteases as pharmacological targets. *Eur J Pharmacol*. 2016;778:44–55. doi: 10.1016/j.ejphar.2015.04.045
  21. Falduto GH, Pfeiffer A, Luker A, Metcalfe DD, Olivera A. Emerging mechanisms contributing to mast cell-mediated pathophysiology with therapeutic implications. *Pharmacol Ther*. 2021;220:107718. doi: 10.1016/j.pharmthera.2020.107718
  22. Shiota N, Rysä J, Kovanen PT, Ruskoaho H, Kokkonen JO, Lindstedt KA. A role for cardiac mast cells in the pathogenesis of hypertensive heart disease. *J Hypertens*. 2003;21:1935–1944. doi: 10.1097/00004872-200310000-00022
  23. Matsuda K, Okamoto N, Kondo M, Arkwright PD, Karasawa K, Ishizaka S, Yokota S, Matsuda A, Jung K, Oida K, et al. Mast cell hyperactivity underpins the development of oxygen-induced retinopathy. *J Clin Invest*. 2017;127:3987–4000. doi: 10.1172/JCI89893
  24. Ninivaggi M, de Laat M, Lancé MMD, Kicken CH, Pelkmans L, Bloemen S, Dirks ML, van Loon LJC, Govers-Riemsag JWP, Lindhout T, et al. Hypoxia induces a prothrombotic state independently of the physical activity. *PLOS ONE*. 2015;10:e0141797. doi: 10.1371/journal.pone.0141797
  25. Palaniyandi SS, Nagai Y, Watanabe K, Ma M, Veeraveedu PT, Prakash P, Kamal FA, Abe Y, Yamaguchi K, Tachikawa H, et al. Chymase inhibition reduces the progression to heart failure after autoimmune myocarditis in rats. *Exp Biol Med Maywood NJ*. 2007;232:1213–1221. doi: 10.3181/0703-RM-85
  26. Tchougounova E, Pejler G, Abrink M. The chymase, mouse mast cell protease 4, constitutes the major chymotrypsin-like activity in peritoneum and ear tissue. A role for mouse mast cell protease 4 in thrombin regulation and fibronectin turnover. *J Exp Med*. 2003;198:423–431. doi: 10.1084/jem.20030671
  27. Aghourian MN, Lemarié CA, Blostein MD. In vivo monitoring of venous thrombosis in mice. *J Thromb Haemost*. 2012;10:447–452. doi: 10.1111/j.1538-7836.2011.04615.x
  28. Canobbio I, Visconte C, Momi S, Guidetti GF, Zarà M, Canino J, Falcinelli E, Gesele P, Torti M. Platelet amyloid precursor protein is a modulator of venous thromboembolism in mice. *Blood*. 2017;130:527–536. doi: 10.1182/blood-2017-01-764910
  29. Terai K, Jin D, Watase K, Imagawa A, Takai S. Mechanism of albuminuria reduction by chymase inhibition in diabetic mice. *Int J Mol Sci*. 2020;21:7495. doi: 10.3390/ijms21207495
  30. Saito MS, Lourenço AL, Kang HC, Rodrigues CR, Cabral LM, Castro HC, Sathier PC. New approaches in tail-bleeding assay in mice: Improving an important method for designing new anti-thrombotic agents. *Int J Exp Pathol*. 2016;97:285–292. doi: 10.1111/iep.12182
  31. Peramo A, Diaz JA. Physical characterization of mouse deep vein thrombosis derived microparticles by differential filtration with nanopore filters. *Membranes*. 2011;2:1–15. doi: 10.3390/membranes2010001
  32. Kakizoe E, Shiota N, Tanabe Y, Shimoura K, Kobayashi Y, Okunishi H. Isoform-selective upregulation of mast cell chymase in the development of skin fibrosis in scleroderma model mice. *J Invest Dermatol*. 2001;116:118–123. doi: 10.1046/j.1523-1747.2001.00165.x
  33. Shen T, Baker K. Venous return and clinical hemodynamics: how the body works during acute hemorrhage. *Adv Physiol Educ*. 2015;39:267–271. doi: 10.1152/advan.00050.2015
  34. Chapin JC, Hajjar KA. Fibrinolysis and the control of blood coagulation. *Blood Rev*. 2015;29:17–24. doi: 10.1016/j.blre.2014.09.003
  35. Semaan W, Desbiens L, Houde M, Labonté J, Gagnon H, Yamamoto D, Takai S, Laidlaw T, Bkaily G, Schwertani A, et al. Chymase inhibitor-sensitive synthesis of endothelin-1 (1–31) by recombinant mouse mast cell protease 4 and human chymase. *Biochem Pharmacol*. 2015;94:91–100. doi: 10.1016/j.bcp.2015.02.001
  36. Khan F, Tritschler T, Kimpton M, Wells PS, Kearon C, Weitz JI, Büller HR, Raskob GE, Ageno W, Couturaud F, et al. Long-term risk for major bleeding during extended oral anticoagulant therapy for first unprovoked venous thromboembolism: a systematic review and meta-analysis. *Ann Intern Med*. 2021;174:1420–1429. doi: 10.7326/M21-1094
  37. Raymond WW, Su S, Makarova A, Wilson TM, Carter MC, Metcalfe DD, Caughey GH.  $\alpha_2$ -macroglobulin capture allows detection of mast cell chymase in serum and creates a reservoir of angiotensin II-generating activity. *J Immunol*. 2009;182:5770–5777. doi: 10.4049/jimmunol.0900127
  38. Diaz JA, Obi AT, Myers DD, Wroblewski SK, Henke PK, Mackman N, Wakefield TW. Critical review of mouse models of venous thrombosis. *Arterioscler Thromb Vasc Biol*. 2012;32:556–562. doi: 10.1161/ATVBAHA.111.244608
  39. Rys RN, Blostein MD, Lemarié CA. Deep vein thrombosis induced by stasis in mice monitored by high frequency ultrasonography. *J Vis Exp JoVE*. 2018:57392. doi: 10.3791/57392
  40. Joglekar MV, Ware J, Xu J, Fitzgerald MEC, Gartner TK. Platelets, glycoprotein Ib-IX, and von Willebrand factor are required for FeCl<sub>3</sub>-induced occlusive thrombus formation in the inferior vena cava of mice. *Platelets*. 2013;24:205–212. doi: 10.3109/09537104.2012.696746
  41. Daley MJ, Murthy MS, Peterson EJ. Bleeding risk with systemic thrombolytic therapy for pulmonary embolism: scope of the problem. *Ther Adv Drug Saf*. 2015;6:57–66. doi: 10.1177/2042098615572333
  42. Kam W, Holmes DN, Hernandez AF, Saver JL, Fonarow GC, Smith EE, Bhatt DL, Schwamm LH, Reeves MJ, Matsouka RA, et al. Association of recent use of non-vitamin K antagonist oral anticoagulants with intracranial hemorrhage among patients with acute ischemic stroke treated with alteplase. *JAMA*. 2022;327:760–771. doi: 10.1001/jama.2022.0948
  43. Li W, Kessinger CW, Orii M, Lee H, Wang L, Weinberg I, Jaff MR, Reed GL, Libby P, Tawakol A, et al. Time-restricted salutary effects of blood flow restoration on venous thrombosis and vein wall injury in mouse and human subjects. *Circulation*. 2021;143:1224–1238. doi: 10.1161/CIRCULATIONAHA.120.049096
  44. Yau JW, Teoh H, Verma S. Endothelial cell control of thrombosis. *BMC Cardiovasc Disord*. 2015;15:130. doi: 10.1186/s12872-015-0124-z
  45. Willems S, Vink A, Bot I, Quax PHA, de Borst GJ, de Vries J-PPM, van de Weg SM, Moll FL, Kuiper J, Kovanen PT, et al. Mast cells in human carotid atherosclerotic plaques are associated with intraplaque microvessel density and the occurrence of future cardiovascular events. *Eur Heart J*. 2013;34:3699–3706. doi: 10.1093/eurheartj/eh186
  46. Payne H, Brill A. Stenosis of the inferior vena cava: a murine model of deep vein thrombosis. *J Vis Exp*. 2017. doi: 10.3791/56697
  47. Dungen H-D, Kober L, Nodari S, Schou M, Otto C, Becka M, Kanefendt F, Winkelmann BR, Gislason G, Richard F, et al. Safety and tolerability of the chymase inhibitor fulacimstat in patients with left ventricular dysfunction after myocardial infarction—results of the CHiARA MIA 1 trial. *Clin Pharmacol Drug Dev*. 2019;8:942–951. doi: 10.1002/cpdd.633
  48. Kanefendt F, Thuß U, Becka M, Boxnick S, Berse M, Schultz A, Otto C. Pharmacokinetics, safety, and tolerability of the novel chymase inhibitor BAY 1142524 in healthy male volunteers. *Clin Pharmacol Drug Dev*. 2019;8:467–479. doi: 10.1002/cpdd.579
  49. Rossing P, Strand J, Avogaro A, Becka M, Kanefendt F, Otto C. Effects of the chymase inhibitor fulacimstat in diabetic kidney disease—results from the CADA DIA trial. *Nephrol Dial Transplant*. 2021;36:2263–2273. doi: 10.1093/ndt/gfaa299

## **SUPPLEMENTAL MATERIAL**

## Data 1. Supplemental Methods

### *Chymase dependent fragmentation of plasmin*

Recombinant mMCP-4 (rmMCP-4) and recombinant CMA-1 (rCMA-1) were produced as pro-forms in our facilities and activated with recombinant mouse cathepsin C (R&D Systems, Minneapolis, MN, USA) as previously described.<sup>35</sup> rmMCP-4 or rCMA-1 was thawed and diluted to a concentration of 20 µg/mL in maturation buffer (50 mM MES, 0.1 % (w/v) BSA, pH 5.5). Active murine cathepsin C was diluted to 20 µg/mL in cathepsin C buffer (50 mM MES, 50 mM NaCl, 5 mM DTT, pH 5.5). Activation was performed by adding equal volumes of recombinant chymase and cathepsin C, adding 50 µg/mL heparin followed by an incubation for 1 h at room temperature. Chymase activation was stopped with 3 mM N-ethylmaleimide (NEM), followed by dilution with assay buffer (20 mM Tris, 2 M KCl, 0.02 % (v/v) Triton X-100, pH 9.0) to bring the recombinant chymase concentration to 2 µg/mL; 5 min was sufficient to completely stop the cathepsin C-dependent reaction. 74 nM of rmMCP-4 or rCMA-1 was pre-incubated with either vehicle or the chymase inhibitor TY-51469 (10 or 300 µM) at 37°C for 20 min, then incubated for 30 min at 37°C with 235 nM of mouse plasmin (Innovative Research Inc., Novi, MI, USA) for rmMCP-4 or 235 nM of human plasmin (Innovative Research Inc., Novi, MI, USA) for rCMA-1. The reaction was stopped with formic acid (FA) (final concentration of 4 % (v/v) in water) and samples were maintained on ice until protein precipitation.

### *In-solution trypsin digestion, purification and desalting of the peptides on C18 columns*

Proteins from *in vitro* cleavage assays were first precipitated by the addition of trichloroacetic acid (TCA) to a final concentration of 10 % (v/v) and incubated for 30 min

at -20°C. Proteins were centrifuged at 10,000 ×g for 15 min. Protein pellets were washed with cold 100 % acetone, air dried, and re-suspended in 50 µL of a solution containing 8 M urea and 10 mM HEPES-KOH (pH 7.4). The protein reduction step was carried out by adding DTT (Thermo Fisher Scientific, Waltham, MA, USA) to a final concentration of 5 mM and heated at 95°C for 2 min, then incubated at room temperature for 30 min. The alkylation of the proteins was carried out by adding iodoacetamide (Sigma-Aldrich, Saint-Louis, MO, USA) to a final concentration of 7.5 mM final before incubating for 20 min at room temperature away from light. Urea concentration was decreased to 2 M by the addition of 150 µL of 50 mM ammonium bicarbonate (NH<sub>4</sub>HCO<sub>3</sub>). The proteins were digested by adding 1 µg Pierce MS-grade trypsin (Thermo Fisher Scientific, Waltham, MA, USA) and incubated overnight at 30°C. Digestion was stopped by adding trifluoroacetic acid (TFA) to a final concentration of 0.2 % (v/v). Peptides were purified with a Pierce C18 100-µL tips column (Thermo Fisher Scientific, Waltham, MA, USA). Briefly, the C18 tip column was first moistened by suctioning 100 µL of 100 % acetonitrile (ACN) three times, then equilibrated by suctioning 100 µL of 0.1 % (v/v) TFA buffer 3 times. Each peptide sample was passed on the balanced C18 tip column by 10 succeeding up-and-downs of 100 µL of the sample. This step was performed twice in order to administer the entire sample on the column. The C18 tip column was then washed with 100 µL of 0.1 % (v/v) TFA buffer 3 times. Elution of peptides was performed in a new low-binding microtube by 10 succeeding up-and-downs with a volume of 100 µL of 50 % (v/v) ACN and 1 % (v/v) FA buffer. This step was carried out 3 times to obtain a final volume of 300 µL. Peptides were then concentrated by a centrifugal evaporator at 65°C until being completely dry (approximately 60 min) and then resuspended in 25 µL of 1 % (v/v) FA



buffer. Peptides were assayed using a NanoDrop spectrophotometer (Thermo Fisher Scientific, Waltham, MA, USA) and read at an absorbance of 205 nm. The peptides were then transferred to a glass vial (Thermo Fisher Scientific, Waltham, MA, USA) and stored at -20°C until analysis by mass spectrometry.

#### *LC-MS/MS analyses*

Trypsin-digested peptides were separated using a Dionex Ultimate 3000 nanoHPLC system. 10 µL of sample (a total of 2 µg) in 1 % (v/v) FA were loaded with a constant flow of 4 µL/min onto an Acclaim PepMap100 C18 column (0.3 mm id x 5 mm, Dionex Corporation). After trap enrichment, peptides were eluted onto an EasySpray PepMap C18 nano column (75 µm x 50 cm, Dionex Corporation) with a linear gradient of 5-35 % solvent B (90 % ACN with 0.1 % FA) over 240 min with a constant flow of 200 nL/min. The HPLC system was coupled to an Orbitrap QExactive mass spectrometer (Thermo Fisher Scientific, Waltham, MA, USA) via an EasySpray source. The spray voltage was set to 2.0 kV and the temperature of the column set to 40°C. Full scan MS survey spectra (m/z 350-1600) in profile mode were acquired in the Orbitrap with a resolution of 70,000 after accumulation of 1,000,000 ions. The 10 most intense peptide ions from the preview scan in the Orbitrap were fragmented by collision-induced dissociation (normalized collision energy 35 % and resolution of 17,500) after the accumulation of 50,000 ions. Maximal filling times were 250 ms for the full scans and 60 ms for the MS/MS scans. Precursor ion charge state screening was enabled and all unassigned charge states as well as singly, 7 and 8 charged species were rejected. The dynamic exclusion list was restricted to a maximum of 500 entries with a maximum retention period of 40 s and a relative mass window of 10 ppm. The lock mass option was enabled for survey scans to improve mass accuracy. Data

were acquired using the Xcalibur software (Thermo Fisher Scientific, Waltham, MA, USA).

#### *Protein Identification by MaxQuant Analysis*

The raw files were analyzed using the MaxQuant software (version 1.6.17.0) and the Uniprot mouse proteome database (07/03/2021, 55 366 entries) or the Uniprot human proteome database (21/03/2020, 75 776 entries), which contain the mouse plasminogen database (UniProtKB - P20918 (PLMN\_MOUSE)) and the human plasminogen database (UniProtKB - P00747 (PLMN\_HUMAN)). The settings used for the MaxQuant analysis were: 4 miscleavages were allowed; minimum peptide length of 6, fixed modification was carbamidomethylation on cysteine; enzymes were Trypsin (K/R) and CMA1 (F/Y); variable modifications included in the analysis were methionine oxidation, protein N-terminal acetylation and protein carbamylation (K, N-terminal). A mass tolerance of 10 ppm was used for precursor ions and a tolerance of 20 ppm was used for fragment ions. Identification values "PSM FDR", "Protein FDR" and "Site decoy fraction" were set to 0.05. Minimum peptide count was set to 1. Label-Free-Quantification (LFQ) was also selected with a LFQ minimal ratio count of 1. The "Second peptides" option was also allowed. Following the analysis, the results were sorted according to several parameters. Proteins positive for at least either one of the "Reverse", "Only.identified.by.site" or "Potential.contaminant" categories were eliminated. Numbering of plasmin/plasminogen amino acids was according to methionine in position 1. Sequences chymase-specific found by LC-MS/MS are depicted in table S2.

### *Measurement of purified Plasmin Enzymatic Activity*

rmMCP-4 or rCMA-1 was activated as described above. 37 nM of rmMCP-4 or rCMA-1 was pre-incubated with either vehicle or TY-51469 (final concentration of 0.1 or 1  $\mu$ M) at 37°C for 20 min, then incubated with 0.12 nM of mouse plasmin or 0.24 nM human plasmin (Innovative Research, Inc., Novi, MI, USA) in 100  $\mu$ L for 24 h at 37°C. Plasmin activity was determined by the hydrolysis rate of 50  $\mu$ M of the fluorogenic substrate, D-Ala-Leu-Lys-7-amino-4-methylcoumarin(AMC) (Sigma Aldrich, Saint-Louis, MO, USA) at 37°C for 1 h. The fluorescence released was measured with an Infinite M1000 spectrophotometer (Tecan Austria GmbH, Grödig, Austria) with  $\lambda_{\text{ex}} = 370$  nm and  $\lambda_{\text{em}} = 460$  nm. A standard curve of AMC was also performed to determine the concentration of the fluorogenic substrate cleavage (nM).

### *Prothrombin Time (PT)*

Blood was collected in citrated tubes by cannulation of the carotid artery and exsanguination of female mice. Citrated tubes were prepared by adding 3.2% (w/v) sodium citrate in a dilution of 1:10 with fresh blood (100  $\mu$ L per 1 mL of blood). Sodium citrate was added as an anticoagulant. Citrated blood samples were centrifuged immediately after collection at 1,000 x g for 10 min at 4°C and at least 100  $\mu$ L of plasma was transferred to another test tube. Measurement of the PT was performed with the Amelung KC1A micro coagulation analyzer (Sigma Diagnostics, St. Louis, MO, USA) at 37°C. In each well, (one well per experiment), a small steering bead was added, and 50  $\mu$ L of plasma was evenly distributed in the bottom of the well. After an incubation time of 60 to 180 s, samples were set for measurement and 100  $\mu$ L of thromboplastin per well was added and mixed. Data were analysed in duplicate.

### *Thromboelastography*

400  $\mu$ L of blood was collected by an intracardiac puncture through the thoracic cage of female mice and quickly placed in a citrated tube. Citrated tubes were prepared by adding 150 mM sodium citrate and diluted 1:10 with fresh blood. 350  $\mu$ L of the citrated blood was then activated with 4% (v/v) of kaolin, which activates the intrinsic coagulation pathway. After activation, 342  $\mu$ L of blood was transferred to TEG 5000 clear disposable cups and pins (Haemonetics, Boston, MA, USA), inserted in the TEG 5000 thromboelastograph hemostasis analyzer system (Haemonetics, Boston, MA, USA) and 18  $\mu$ L  $\text{CaCl}_2$  (200 mM) was added. Results were acquired with the Axon axoscope 10.4 acquisition system (Molecular devices, Sunnyvale, CA, USA) and the analysis was performed with clampfit 10.4 (Molecular devices, Sunnyvale, CA, USA).

### *Quantification of histology and immunostaining*

The images were analysed with Image J with Immunohistochemistry toolbox plugin. Both the positive cells numbers and positive areas for Toluidine blue and mMCP-4 for the same total pixel area for each vessel analysed are shown.



**Table S1 – Histology and Immunostaining scores**

	<b>mMCP-4 positive cells</b>	<b>mMCP-4 positive area (%)</b>	<b>TB positive cells</b>	<b>TB positive area (%)</b>	<b>Total area (pixels)</b>
<b>WT Healthy</b>	234	2.61	20	1.437	5041312
<b>WT DVT</b>	633	11.54	7	0.311	5041312
<b>mMCP-4 KO DVT</b>	0	0	5	0.395	5041312

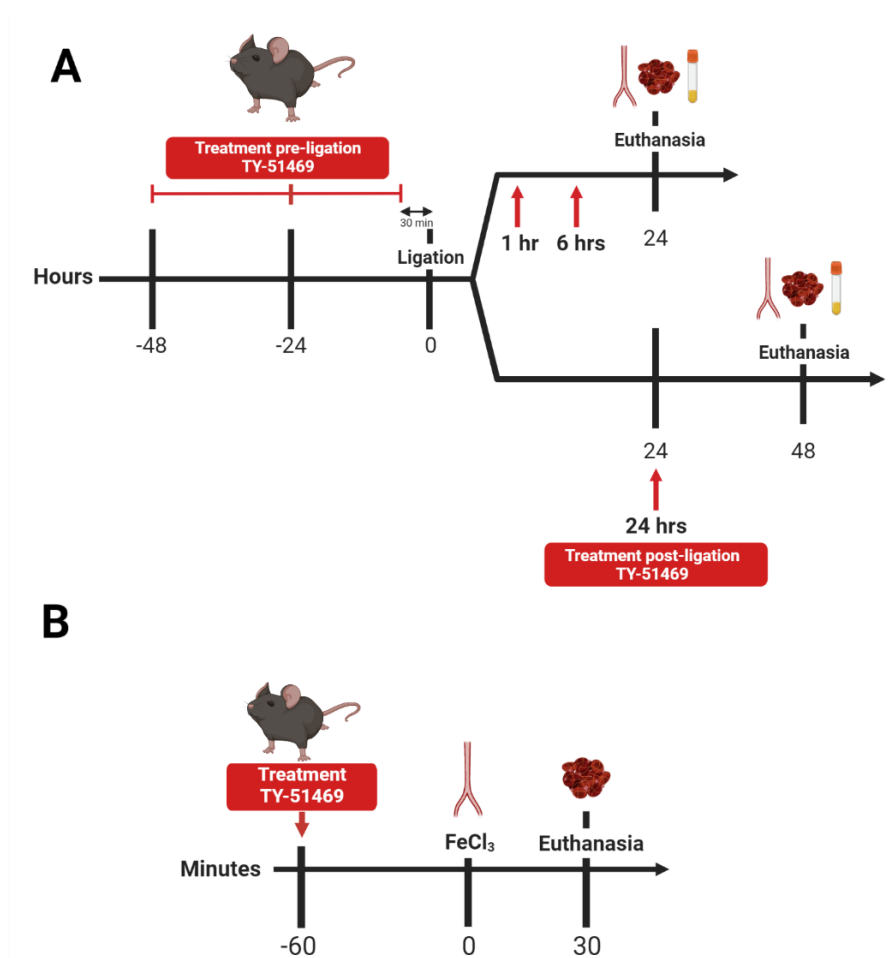
TB: Toluidine blue staining

1

2 **Table S2 - Identification of rCMA-1 cleavage sites in human plasmin using trypsin digestion and cleavage product**  
3 **identification by LC-MS/MS.**

Cleavage site	Sequence	Intensity											
		Plasmin only				Plasmin + rCMA-1				Plasmin + rCMA-1 + TY-51469			
F711	<i>R</i> - <u>TECFITGWGETQGTF</u> -G	0	0	0	0	1.19E+09	8.67E+08	2.88E+08	1.77E+08	0	8.45E+07	0	0
F711'	<i>K</i> - <u>VIPACLPSPNYVVADRTECFITGWGETQGTF</u> -G	0	0	0	0	2.57E+08	3.68E+08	7.79E+06	5.40E+06	0	0	0	0
F799	<i>F</i> - <u>VTWIEGVMR</u> -N	0	0	0	0	2.17E+08	3.13E+08	3.67E+08	2.97E+08	0	0	0	0
F602	<i>F</i> - <u>GMHFCGGTLISPEWVLTAHCLK</u> -S	0	0	0	0	2.00E+08	4.34E+08	0	0	0	0	0	0
F565	<i>R</i> - <u>KLYDYCDVPOCAAPSF</u> -R	0	0	0	0	0	4.26E+08	2.55E+07	0	0	0	0	0
F224	<i>K</i> - <u>TMSGLECOAWDSQSPHAHGYIPSK</u> -P	0	0	0	0	0	7.94E+07	0	0	0	1.86E+07	0	0
F246	<i>F</i> - <u>TTDPNKRWELCDIPR</u> -C	0	0	0	0	0	7.79E+06	0	3.18E+07	0	0	0	0

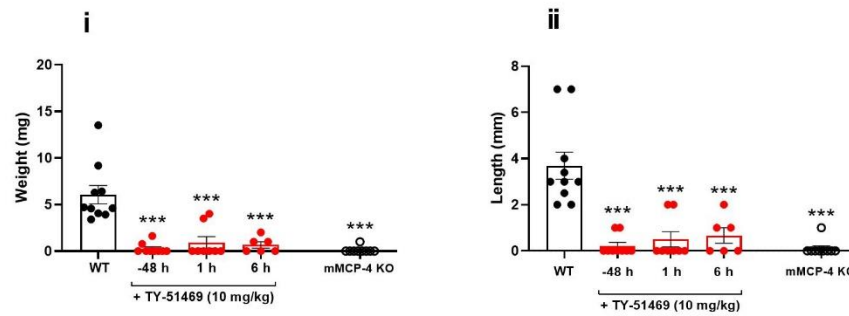
4 Peptide identified after *in vitro* trypsin digestion and LC-MS/MS analysis of plasmin fragments generated by rCMA-1 cleavage are underlined. 4 independent experiments were  
5 tested for each condition. F711 and F711' represent the same cleavage site but two peptides were detected due to a mis cleavage by trypsin. rCMA-1-specific cleavage are in **bold**  
6 **letters**, trypsin-specific cleavage are in *italic* and **bold** letters and trypsin miscleavage are represented in *italic* letters.



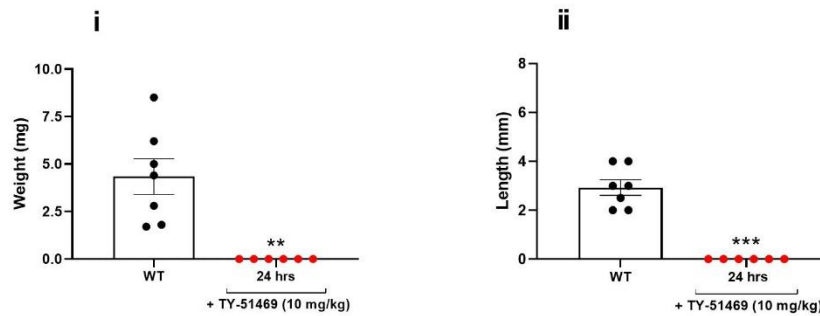
8

**Figure S1 - Schematic experimental design.** A) For the partial ligation protocol, TY-51469 was administered at 10 mg/kg (intra-peritoneal, IP), either pre-ligation (consecutive injections at 48 h, 24 h and 30 min pre-ligation) or as a single injection 1, 6 or 24 h post-DVT. Thrombus formation was evaluated 24 or 48 h post-ligation. B) For the ferric chloride (FeCl<sub>3</sub>)-induced-endothelium insult model, TY-51469 was administered at 10 mg/kg IP 1 h pre-anesthesia of the animal. After the FeCl<sub>3</sub> insult on the IVC, thrombus assessment was completed 30 min later. Created with BioRender.com.

## A 24 hrs



## B 48 hrs



## C

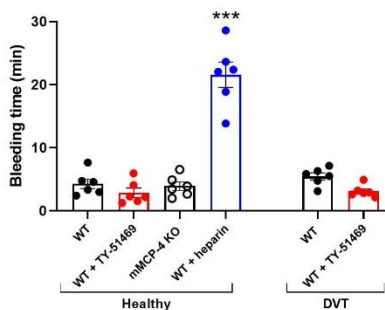


**Figure S2 - No sex difference was observed on the efficacy of a chymase inhibitor to protect against or resolve a deep vein thrombosis (DVT).** Female WT mice  $\pm$  10 mg/kg TY-51469 intra-peritoneal (IP) and female mMCP-4 KO mice were subjected to an inferior vena cava (IVC) stenosis for A) 24 h or B) 48 h. Morphometric parameters of thrombi are measured as i) weight (mg) and ii) length (mm). Note the efficacy of TY-51469 to prevent or resolve DVT in female mice subjected to a IVC stenosis, as also shown in male mice (Figure 3). C) There were no differences in female mice bleeding times between WT mice

$\pm 10$  mg/kg TY-51469, mMCP-4 KO or DVT WT mice  $\pm 10$  mg/kg TY-51469. 300 U/kg heparin-treated female WT mice were used as positive controls. Each group represents the mean  $\pm$  S.E.M. (n = 6-16). \*\* P<0.01; \*\*\* P<0.001 compared with the WT control group.

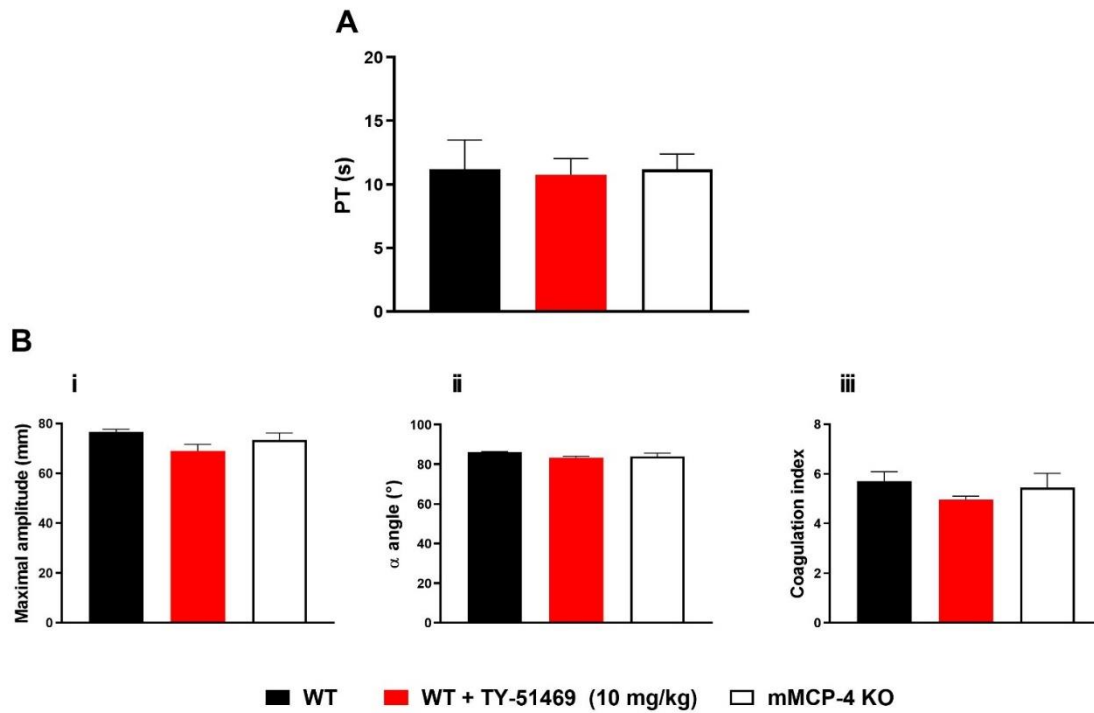


**Figure S3 - Chymase inhibition does not affect mice coagulation parameters *in vitro*.**

A) Prothrombin times (PT) were measured in plasma from female WT mice  $\pm$  10 mg/kg TY-51469 intra-peritoneal (IP) treatment, and in chymase-deficient (mMCP-4 KO) female mice. B) Thromboelastography of blood samples extracted from vehicle- or TY-51469-treated female WT mice, or from mMCP-4 KO mice reveals no difference in i) maximal amplitude, ii) alpha angle or iii) coagulation index. Each group of mice represents the mean  $\pm$  S.E.M. (n = 5-6).



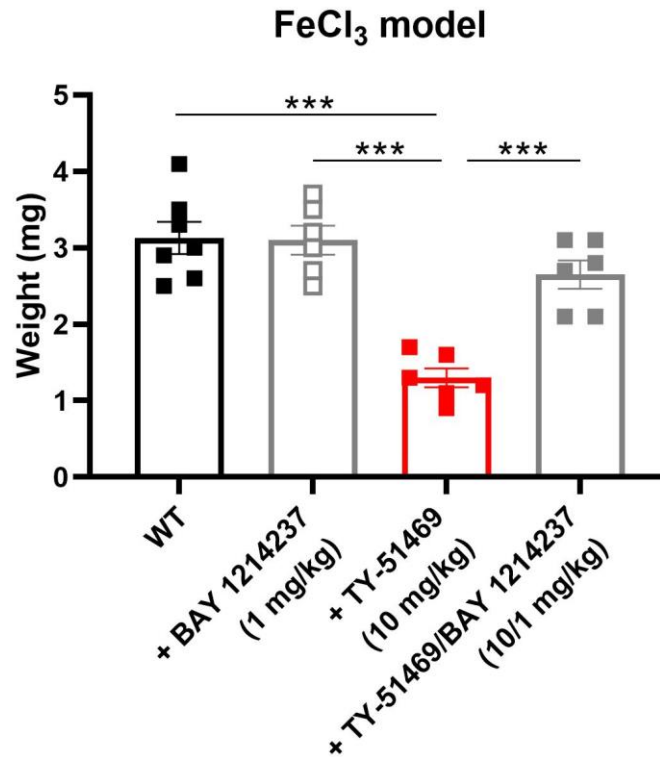


**Figure S4 - The plasmin inhibitor BAY 1214237 abolishes the anti-DVT properties of TY-51469 in the mouse ferric chloride ( $\text{FeCl}_3$ ) model.** Weight of thrombi obtained after the  $\text{FeCl}_3$  insult model 30 min post-damage, from male WT mice treated 1 h pre-insult, with vehicle, BAY 1214237 (1 mg/kg), TY-51469 (10 mg/kg) or a combination of both inhibitors. Each group represents the mean  $\pm$  S.E.M. (n = 6-7). \*\*\*  $P < 0.001$  compared with the WT control group.

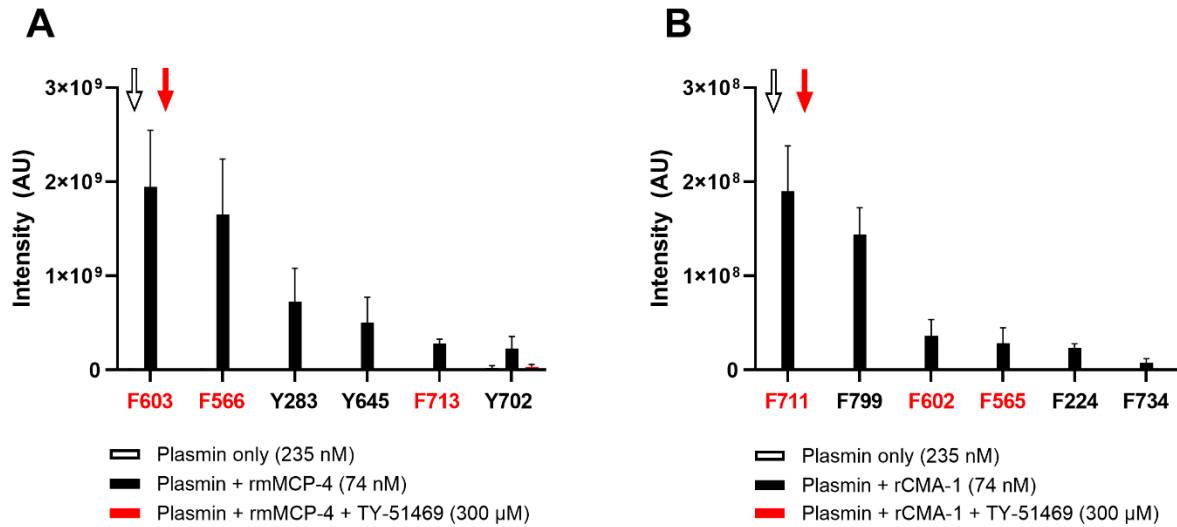


**Figure S5 - Mouse (rmMCP-4) or human (rCMA-1) recombinant chymase cleave murine or human plasmin respectively, with homologous cleavage sites. A, B)** Identification of recombinant murine (A) or human (B) chymase cleavage sites in plasmin using trypsin digestion and cleavage product identification by Liquid Chromatography with tandem mass spectrometry (LC-MS/MS), represented as arbitrary intensity. Homologous cleavage sites in human and mouse plasmin are indicated in red. Each column represents the mean  $\pm$  S.E.M. (n = 4).